

The Masses and Accretion Rates of White Dwarfs in Classical and Recurrent Novae

Michael M. Shara^{1,2}, Dina Prialnik³, Yael Hillman^{1,4} and Attay Kovetz⁵

ABSTRACT

Models have long predicted that the frequency-averaged masses of white dwarfs in Galactic classical novae are twice as large as those of field white dwarfs. Only a handful of dynamically well-determined nova white dwarf masses have been published, leaving the theoretical predictions poorly tested. The recurrence time distributions and mass accretion rate distributions of novae are even more poorly known. To address these deficiencies, we have combined our extensive simulations of nova eruptions with the Strophe et al. (2010) and Schaefer (2010) databases of outburst characteristics of Galactic classical and recurrent novae to determine the masses of 92 white dwarfs in novae. We find that the mean mass (frequency averaged mean mass) of 82 Galactic classical novae is 1.06 (1.13) M_{\odot} , while the mean mass of 10 recurrent novae is $1.31 M_{\odot}$. These masses, and the observed nova outburst amplitude and decline time distributions allow us to determine the long-term mass accretion rate distribution of classical novae. Remarkably, that value is just $1.3 \times 10^{-10} M_{\odot}/\text{yr}$, which is an order of magnitude smaller than that of cataclysmic binaries in the decades before and after classical nova eruptions. This predicts that old novae become low mass transfer rate systems, and hence dwarf novae, for most of the time between nova eruptions. We determine the mass accretion rates of each of the 10 known Galactic RN, finding them to be in the range 10^{-7} - $10^{-8} M_{\odot}/\text{yr}$. We are able to predict

¹Department of Astrophysics, American Museum of Natural History, Central Park West and 79th Street, New York, NY 10024-5192, USA

²Institute of Astronomy, University of Cambridge, Madingley Road, Cambridge CB3 0HA, United Kingdom

³Department of Geosciences, Tel Aviv University, Ramat Aviv, Tel Aviv 69978, Israel

⁴Department of Particle Physics and Astrophysics, Weizmann Institute of Science, 76100 Rehovot, Israel

⁵School of Physics and Astronomy, Faculty of Exact Sciences, Tel-Aviv University, Tel Aviv, Israel

the recurrence time distribution of novae and compare it with the predictions of population synthesis models.

Subject headings: novae, cataclysmic variables, white dwarfs

1. Introduction

Novae are powered by thermonuclear runaways (TNRs) in the hydrogen-rich envelopes of white dwarf (WD) stars (Starrfield et al. 1975; Prialnik et al. 1978). Those envelopes are accreted from brown dwarf, red dwarf, subgiant or red giant companions in the stellar binary systems known as cataclysmic variables (CVs). WD envelopes become increasingly electron degenerate as their masses increase. Once a critical pressure is reached, the timescale for nuclear energy generation at the base of a WD hydrogen-rich envelope becomes smaller than the timescale to transport away that energy. A TNR inevitably ensues (Shara 1981a), with the resulting nova reaching maximum magnitude in the range $M = -5$ to -10.7 (Shafter et al. 2009).

The degenerate equation of state of a WD ensures that its radius decreases and its gravitational potential greatly increases as its mass increases (Chandrasekhar 1931, 1935). Thus, with increasing WD mass, less hydrogen can be accreted onto a WD before a TNR occurs (Shara 1981a). All other things being equal, lower mass envelopes can be ejected faster than those of higher mass, so nova TNRs on massive WDs should eject their envelopes, and begin to decline in brightness, faster than those on low mass WDs. Thus if WD mass was the *only* free parameter in nova binaries then novae would be luminous, well-understood standard candles displaying negligible scatter (Shara 1981a; Livio 1992). The WD mass would be tightly correlated with, and directly measurable from the rate at which a nova declines in brightness.

In fact, nova eruptions display a 3 magnitude scatter about the so-called Maximum Magnitude - Rate of Decline Relation (MMRD) (Prialnik & Kovetz 1995; Yaron et al. 2005; Hachisu & Kato 2010), rendering the MMRD nearly useless as a distance indicator (Ferrarese et al. 2003; Kasliwal et al. 2011; Shara et al. 2017). Just as important, the MMRD relation cannot be used to determine WD masses.

Several factors, in addition to WD mass, influence each nova outburst (Starrfield et al. 1975; Shara et al. 1980). These are the accretion rate onto the WD and the resulting envelope mass (Paczynski & Zytkov 1978; Prialnik et al. 1982); the WD luminosity (Prialnik & Kovetz 1995; Yaron et al. 2005); its chemical composition (He, CO or ONe), and the chemical composition of the accreted matter (H-rich or He) (Faulkner et al. 1972; Kovetz & Prialnik 1985;

Starrfield et al. 1986). For primarily hydrogen-accreting, CO WDs, the accreted mass is the next most important parameter after the WD mass in determining a nova’s outburst properties (Shara et al. 2017).

There is compelling evidence that the mass of the WD in a CV is not static in time. The highly CNO or Ne-enriched ejecta of some novae demonstrate that WD material is being ablated during some nova eruptions (Williams et al. 1978; Gallagher et al. 1980; Williams 1982; Gehrz et al. 2008). The existence of a WD in nova M31N 2008-12a (hereafter M31-12a) which recurs at least annually (Henze et al. 2015) demands a WD close to the Chandrasekhar mass (Kato et al. 2014). No trace of neon is seen in ultraviolet spectra of its ejecta (Darnley et al. 2017). The CO WD in RS Oph is nearly as massive ($\sim 1.3M_{\odot}$) (Mikolajewska & Shara 2017). Since CO WDs cannot be born with masses larger than $\sim 1.1M_{\odot}$ (Iben & Tutukov 1985; Ritossa et al. 1996), the underlying WDs in RS Oph and M31-12a have likely experienced significant mass growth since their births.

The latter results suggest that WDs in some nova systems may approach the Chandrasekhar mass, and may produce type Ia supernovae (Whelan & Iben 1973; Canal et al. 1996; Han & Podsiadlowski 2004; Maoz et al. 2014). Understanding the evolution of WD masses in CVs, and their resulting connections to SNIa is thus an important, though challenging task. While the mass distribution of single WDs near the Sun is sharply peaked at $\sim 0.6M_{\odot}$ (Bergeron et al. 1992; Kepler et al. 2016), population synthesis models (Ritter et al. 1991; Politano 1996; Nelson et al. 2004; Chen et al. 2016) predict a much wider range of nova WD masses. Ritter et al. (1991) and Nelson et al. (2004) find frequency-averaged masses of WDs in nova systems that are $1.14 \pm 0.10 M_{\odot}$ and $0.95 \pm 0.15 M_{\odot}$, respectively. They note that these values are in good agreement with the observational estimate of $0.90 M_{\odot}$ (Ritter et al. 1991). This latter WD mass estimate was based on 8 novae; none of those WD masses were dynamically determined.

In fact, accurate, dynamically-determined measurements of nova WD masses and frequency-averaged WD masses are extremely difficult to make, and few in number, because the WD radial velocities are almost always masked by their accretion disks (Young & Schneider 1980; Smith et al. 1998). Sion (1999) has summarised the range of observational data and assumptions that goes into determining nova WD masses (including parameters of emission-line profiles, velocity width at half or mean intensity, rms line widths, and velocity separation of doubled emission peaks), as well as the assumption of Roche geometry and an empirical mass-radius relation for the secondary stars. The host of assumptions and approximations, and the small number of nova systems for which these procedures have been carried out, suggest that one of the most direct and critical predictions of stellar binary population synthesis models - the mass distribution of WDs in novae - has not been adequately tested.

The theoretically-predicted mass transfer rate and recurrence time distributions are even less well-determined.

The goal of this paper is to demonstrate a methodology for determining the mass of a WD in a nova CV, utilizing only our extensive simulations of novae combined with observables that are straightforward to measure for any nova. Extensions of the methodology also yield the mass transfer rate and recurrence time distributions of Galactic novae. We apply this methodology to determine the masses and mass transfer rates of 82 WDs in classical novae (CN), and another 10 in recurrent novae (RNe). We also derive the recurrence time distribution for those same 82 CN WDs. This is by far the largest sample of novae for which these parameters have been derived in a uniform and consistent manner. The results enable the strongest tests to date of nova population synthesis models’ predictions.

In Section 2 we summarize our nova models and the relationships between model parameters — WD mass and accretion rate — and the resulting nova characteristics, such as nova outburst amplitude, envelope mass and decline time, which enable the determination of WD masses and accretion rates based on observations. In Section 3 we describe the observations of Galactic RNe and CN which serve as the databases for this study. In section 4 we use the model-derived relationships to determine the masses of the WDs in the databases, as well as the accretion rates and recurrence times and their distributions. We compare the results with the few dynamically measured nova WD masses, and with the predictions of nova WD masses from population synthesis models. We also compare our WD mass results with those of derived from a completely different methodology - nova atmospheric models. In section 5 we determine and discuss the *true* WD mass and mass accretion rate distributions in Galactic novae. Our conclusions are summarized in section 6.

2. Nova Models: relationships between nova characteristics

One of the most extensive and widely used ensembles of nova models is that of Yaron et al. (2005). White dwarf masses of 0.4, 0.65, 1.00, 1.25 and 1.40 M_{\odot} and core temperatures of 10, 30 and 50 MKelvins, were allowed to accrete solar composition matter at rates of $10^{-6}, 10^{-7}, 10^{-8}, 10^{-9}, 10^{-10}, 10^{-11}$, and $10^{-12} M_{\odot}/\text{yr}$. Details of the hydrodynamic Lagrangian stellar evolution code, including the opacities, nuclear reactions network, mass-loss algorithm, diffusion and accretion heating, and convective fluxes are described in detail in Prialnik & Kovetz (1995) and Yaron et al. (2005). To these we add the models from Hillman et al. (2016) which more densely cover the parameter space of WDs accreting at the very high rates (3×10^{-8} to $6 \times 10^{-7} M_{\odot}/\text{yr}$), which can grow WD masses considerably.

Each of these models predicts the total mass accreted before a TNR, and the outburst characteristics of each of the resulting novae. In particular, we emphasize that the amplitude in visual magnitudes of the outburst A , as well as the duration of the mass-loss phase t_{m-l} are calculated by Yaron et al. (2005). These two parameters are directly observable for many Galactic novae. They enable us to match models specified by just three parameters - white dwarf mass, core temperature and mass accretion rate - with well observed Galactic novae, regardless of their often poorly-determined distances. Of the three model parameters, the least important one by far (in the sense that results are affected by it to a much lesser extent) is the core temperature. We adopt the intermediate WD core temperature of 30 MKelvins in the Yaron et al. (2005) models, and use just the two independent model parameters, M_{WD} and \dot{M} . The results used are given in Tables 1 and 2.

Table 1: Nova outburst amplitudes A derived from models (Yaron et al. 2005)

	M_{WD}	$0.65M_{\odot}$	$1.00M_{\odot}$	$1.25M_{\odot}$	$1.40M_{\odot}$
$\log \dot{M}$					
-8		9.5	9.4	9.0	8.4
-9		12.0	12.0	11.6	11.0
-10		16.2	14.4	14.3	13.6
-11		15.2	15.3	15.4	15.3

Table 2: Mass loss times t_{m-l} (log(days)) derived from models (Yaron et al. 2005)

	M_{WD}	$0.65M_{\odot}$	$1.00M_{\odot}$	$1.25M_{\odot}$	$1.40M_{\odot}$
$\log \dot{M}$					
-8		3.09	2.20	1.51	0.67
-9		2.83	2.15	1.50	0.11
-10		2.68	2.07	1.34	0.18
-11		1.57	1.01	0.31	-0.73

3. Nova Observations: outburst amplitudes and decline times

The largest uniform compilation of Galactic nova light curves is that of Strope et al. (2010). The detailed observational characteristics of 93 novae - including the outburst amplitudes A and times t_2 to decline by two magnitudes from peak brightness - are summarised

from almost 230,000 individual measured magnitudes. The largest uniform compilation of recurrent nova (RN) light curves is that of Schaefer (2010).

High accretion rates on massive WDs can accumulate critical envelope masses on timescales as short as years (Yaron et al. 2005). This is the source of the Recurrent Novae (RNe), which have massive WDs and inter-eruption intervals of a century or less. RNe have recently been estimated to comprise 25% of all novae (Pagnotta & Schaefer 2014). Examples include M31-12a and RS Oph. The extraordinary recurrent nova M31N 2008-12a in the Andromeda galaxy, which erupts every year (Henze et al. 2015) and fades by 2 magnitudes in just 1.65 days (Darnley et al. 2016) must host a WD with a mass within a few percent of the Chandrasekhar mass. The mass of the WD in RS Oph must lie in the range $1.3 \pm 0.10 M_{\odot}$ (Mikolajewska & Shara 2017), while that in TCrB is most likely $\sim 1.2 M_{\odot}$ (Belczynski & Mikolajewska 1998).

In Table 1 we list the novae that will serve as our database, and their outburst amplitudes A and times of decline by two magnitudes t_2 . The distribution of decline times t_2 is shown in Fig.1.

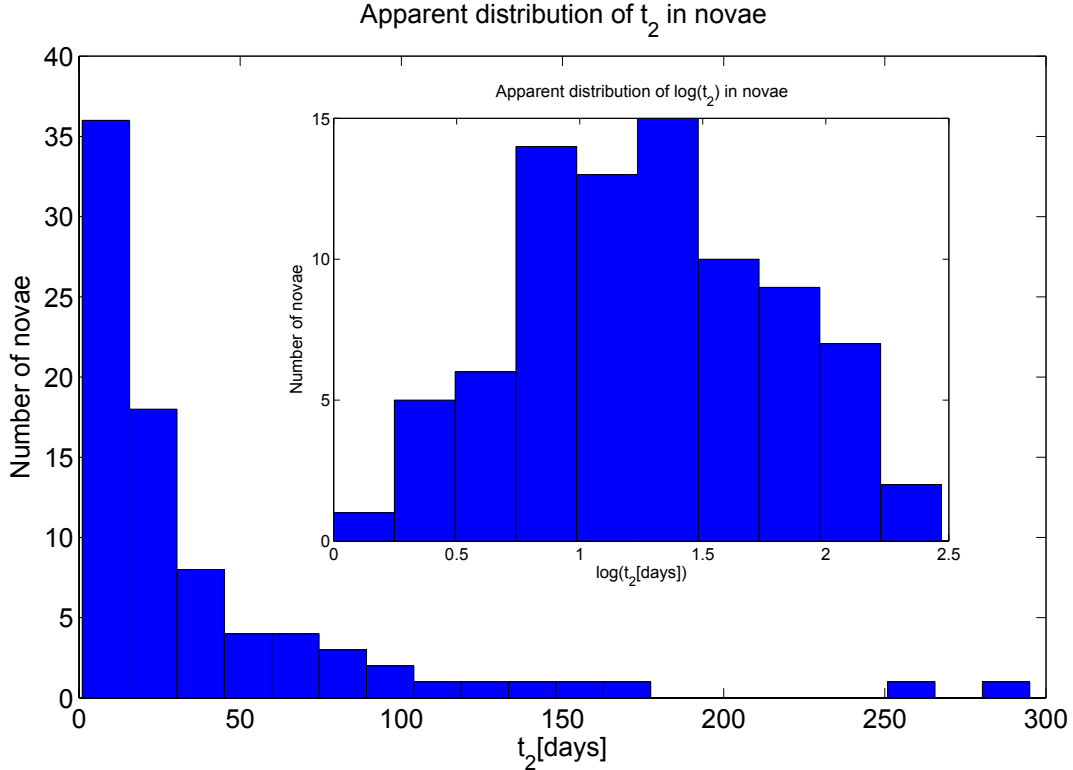


Fig. 1.— The apparent distribution of decline times t_2 for the CN sample.

4. The masses of WDs in Galactic CN and RNe and their accretion rates

As mentioned in Section 2, the grid of models over the (M_{WD}, \dot{M}) space for a given WD core temperature yields, among other characteristics, the outburst amplitudes A and the mass-loss times of novae t_{m-l} . Observations yield, among other characteristics, the outburst amplitudes A and the times of decline by two magnitudes t_2 , as mentioned in Section 3. The working assumption of our study will be that the observationally derived t_2 and the model-derived mass loss time t_{m-l} are identical. We denote both by t_{dec} ,

$$t_2 \equiv t_{\text{dec}} \equiv t_{m-l} .$$

Ideally, we would require from observations and models both the duration of the mass-loss phase t_{m-l} and the visual decline time t_2 . Unfortunately, self-consistent evolutionary models provide the mass loss phase duration accurately, together with its dependence on the WD mass and accretion rate, while observations provide accurately the visual decline time. Fortunately, however, these times are closely connected, as shown analytically in the Appendix of Shara (1981a). The maximal luminosity of a nova in the visible band is obtained when the envelope has become extended enough for mass loss to begin. Near the end of mass loss, the WD contracts rapidly, the luminosity shifts to shorter wavelengths, and the visual luminosity starts declining. This is why we have adopted the earlier decline time obtained from observations, that is, t_2 rather than t_3 , t_4 , etc., as the closest to the mass-loss time derived from modeling.

Now, we interpolate in the grid of models given in Tables 1 and 2, using second-order polynomials, to obtain functions $A(M_{\text{WD}}, \dot{M})$ and $t_{\text{dec}}(M_{\text{WD}}, \dot{M})$. These relations are then inverted for each pair of observables A and t_{dec} in the sample of Strobe et al. (2010), to determine both the WD mass $M_{\text{WD}}(A, t_{\text{dec}})$ and accretion rate $\dot{M}(A, t_{\text{dec}})$ of the corresponding nova (a similar procedure was already used by Prialnik & Kovetz (1995)). The results are given in Table 3. We omitted three CN from the sample of 85 CN in Strobe et al. (2010): V445 Pup (which is an eruption of a helium envelope, rather than a TNR in a hydrogen-rich envelope), as well as V888 Cen and CP Pup. The amplitude A of V888 Cen is very small, falling near the limits of the A range (similar to those on RNe), while that of CP Pup is very large, so that the WD masses could not be determined.

For RNe, we again need two observables that can be fitted by model results, so that the relations can be inverted to obtain the WD mass and the accretion rate. Since the ranges of amplitudes and decline times are not sufficiently wide to provide reliable fit functions, we use two other observables, which are available for RNe: the flash duration f (i.e. the time from first brightening to final decline) and the average recurrence period p_{rec} , both of which we take from Schaefer (2010). We thus derive new fit formulae $f(M_{\text{WD}}, \dot{M})$ and $p_{\text{rec}}(M_{\text{WD}}, \dot{M})$

Table 3: CN: WD masses and accretion rates from observations (Strope et al. 2010) and models

Observations				Modeling			
Year	Nova	A(mag)	t_2 (days)	$M_{\text{WD}}(M_{\odot})$	$\log \dot{M}(M_{\odot}/\text{yr})$	$p_{\text{rec}}(\text{yr})$	$m_{\text{acc}}(M_{\odot})$
1986	OS And	11.0	11	1.16	-8.81	6.91E+03	1.07E-05
1925	DO Aql	9.5	295	0.62	-8.16	1.68E+04	1.16E-04
1936	V356 Aql	11.3	127	0.85	-8.94	2.85E+04	3.26E-05
1945	V528 Aql	11.6	16	1.14	-9.07	1.58E+04	1.34E-05
1918	V603 Aql	12.2	5	1.24	-9.33	1.07E+04	4.97E-06
1970	V1229 Aql	11.5	18	1.12	-9.03	1.54E+04	1.45E-05
1982	V1370 Aql	10.3	15	1.13	-8.51	4.14E+03	1.29E-05
1993	V1419 Aql	13.4	25	1.08	-9.85	1.12E+05	1.57E-05
1995	V1425 Aql	12.0	27	1.09	-9.24	3.08E+04	1.75E-05
1999	V1493 Aql	10.9	9	1.18	-8.77	5.38E+03	9.17E-06
1999	V1494 Aql	13.0	8	1.20	-9.68	3.44E+04	7.22E-06
1891	T Aur	10.4	80	0.93	-8.55	9.05E+03	2.54E-05
1993	V705 Cas	10.7	33	1.05	-8.68	9.45E+03	1.97E-05
1995	V723 Cas	8.6	263	0.77	-7.77	1.51E+03	2.55E-05
1986	V842 Cen	10.9	43	1.02	-8.77	1.28E+04	2.18E-05
1991	V868 Cen	11.2	31	1.06	-8.90	1.53E+04	1.93E-05
2001	V1039 Cen	11.7	25	1.09	-9.11	2.23E+04	1.71E-05
1995	BY Cir	10.5	35	1.04	-8.60	7.84E+03	1.99E-05
1999	DD Cir	12.6	5	1.24	-9.50	1.52E+04	4.76E-06
1981	V693 CrA	14	10	1.15	-10.11	1.19E+05	9.24E-06
1920	V476 Cyg	14.3	6	1.18	-10.24	1.14E+05	6.53E-06
1970	V1330 Cyg	7.6	161	0.91	-7.34	2.67E+02	1.22E-05
1975	V1500 Cyg	16.0	2	1.09	-10.98	6.72E+05	7.09E-06
1978	V1668 Cyg	13.5	11	1.16	-9.89	7.39E+04	9.42E-06
1986	V1819 Cyg	7.7	95	0.97	-7.38	2.88E+02	1.19E-05
1992	V1974 Cyg	12.6	19	1.12	-9.50	4.44E+04	1.39E-05
2001	V2274 Cyg	8.5	22	1.13	-7.73	5.09E+02	9.51E-06
2001	V2275 Cyg	11.5	3	1.27	-9.03	3.37E+03	3.15E-06
2006	V2362 Cyg	12.9	9	1.19	-9.63	3.45E+04	8.01E-06
2007	V2467 Cyg	11.6	8	1.20	-9.07	9.53E+03	8.09E-06
2008	V2491 Cyg	12.5	4	1.26	-9.46	1.11E+04	3.82E-06
1967	HR Del	8.5	167	0.84	-7.73	1.03E+03	1.92E-05
1912	DN Gem	12	16	1.14	-9.24	2.29E+04	1.30E-05

Table 3: CN: WD masses and accretion rates (*cont.*)

Observations				Modeling			
Year	Nova	A(mag)	t_2 (days)	$M_{\text{WD}}(M_{\odot})$	$\log \dot{M}(M_{\odot}/\text{yr})$	$p_{\text{rec}}(\text{yr})$	$m_{\text{acc}}(M_{\odot})$
1934	DQ Her	12.7	76	0.95	-9.55	8.87E+04	2.51E-05
1960	V446 Her	11.3	20	1.11	-8.94	1.36E+04	1.55E-05
1963	V533 Her	12.0	30	1.07	-9.24	3.24E+04	1.84E-05
1987	V827 Her	10.6	21	1.10	-8.64	6.92E+03	1.59E-05
1991	V838 Her	13.8	1	1.35	-10.02	6.44E+03	6.09E-07
1936	CP Lac	13.0	5	1.24	-9.68	2.21E+04	4.63E-06
1950	DK Lac	7.9	55	1.03	-7.47	3.38E+02	1.15E-05
1939	BT Mon	7.6	118	0.95	-7.34	2.57E+02	1.15E-05
1998	LZ Mus	9.5	4	1.27	-8.16	4.15E+02	2.85E-06
1919	V849 Oph	11.2	140	0.82	-8.90	2.80E+04	3.54E-05
1988	V2214 Oph	12.0	60	0.99	-9.24	4.23E+04	2.41E-05
1991	V2264 Oph	11.0	22	1.10	-8.81	1.06E+04	1.64E-05
1993	V2295 Oph	11.7	9	1.19	-9.11	1.15E+04	8.83E-06
1994	V2313 Oph	12.5	8	1.20	-9.46	2.15E+04	7.44E-06
2002	V2540 Oph	12.9	66	0.96	-9.63	1.02E+05	2.37E-05
1901	GK Per	12.8	6	1.22	-9.59	2.19E+04	5.60E-06
1925	RR Pic	11.2	73	0.95	-8.90	2.05E+04	2.59E-05
1991	V351 Pup	13.2	9	1.19	-9.76	4.63E+04	7.96E-06
2004	V574 Pup	10.2	12	1.15	-8.47	3.19E+03	1.09E-05
1977	HS Sge	13.5	15	1.13	-9.89	9.20E+04	1.17E-05
1936	V732 Sgr	9.6	65	0.95	-8.21	3.41E+03	2.13E-05
1977	V4021 Sgr	9.1	56	0.98	-7.99	1.78E+03	1.82E-05
1991	V4160 Sgr	12	2	1.30	-9.24	3.25E+03	1.85E-06
1992	V4169 Sgr	9.1	24	1.09	-7.99	1.30E+03	1.33E-05
1999	V4444 Sgr	13.4	5	1.23	-9.85	3.29E+04	4.64E-06
1998	V4633 Sgr	11.3	17	1.13	-8.94	1.23E+04	1.41E-05
2001	V4643 Sgr	8.3	3	1.40	-7.64	5.32E+00	1.21E-07
2001	V4739 Sgr	10.8	2	1.30	-8.72	1.04E+03	1.97E-06
2001	V4740 Sgr	11.3	18	1.12	-8.94	1.28E+04	1.46E-05
2002	V4742 Sgr	10.1	9	1.18	-8.42	2.28E+03	8.62E-06
2002	V4743 Sgr	11.8	6	1.22	-9.16	8.89E+03	6.18E-06
2003	V4745 Sgr	9.7	79	0.92	-8.25	4.04E+03	2.28E-05
2004	V5114 Sgr	12.9	9	1.19	-9.63	3.45E+04	8.01E-06
2005	V5115 Sgr	10.1	7	1.20	-8.42	1.83E+03	6.91E-06
2005	V5116 Sgr	8.4	12	1.22	-7.69	1.97E+02	4.06E-06

Table 3: CN: WD masses and accretion rates (*cont.*)

Observations				Modeling			
Year	Nova	A(mag)	t_2 (days)	$M_{\text{WD}}(M_{\odot})$	$\log \dot{M}(M_{\odot}/\text{yr})$	$p_{\text{rec}}(\text{yr})$	$m_{\text{acc}}(M_{\odot})$
1992	V992 Sco	9.5	100	0.89	-8.16	3.38E+03	2.33E-05
2004	V1186 Sco	8.3	12	1.24	-7.64	1.46E+02	3.34E-06
2004	V1187 Sco	8.2	10	1.28	-7.60	6.28E+01	1.58E-06
2005	V1188 Sco	10.1	11	1.16	-8.42	2.67E+03	1.01E-05
1975	V373 Sct	12.2	47	1.02	-9.33	4.70E+04	2.19E-05
1989	V443 Sct	11.5	33	1.06	-9.03	2.10E+04	1.97E-05
1970	FH Ser	12.3	49	1.02	-9.37	5.25E+04	2.22E-05
1978	LW Ser	11.1	32	1.06	-8.85	1.40E+04	1.96E-05
1999	V382 Vel	13.8	6	1.21	-10.02	6.13E+04	5.80E-06
1968	LV Vul	10.8	20	1.11	-8.72	8.28E+03	1.56E-05
1976	NQ Vul	11.0	21	1.10	-8.81	1.04E+04	1.60E-05
1984	PW Vul	10.5	44	1.01	-8.60	8.49E+03	2.16E-05
1984	QU Vul	12.6	20	1.12	-9.50	4.58E+04	1.43E-05
1987	QV Vul	10.9	37	1.04	-8.77	1.21E+04	2.07E-05

based on the denser grid of RNe models calculated by Hillman et al. (2016) for a WD core temperature of 30 MKelvins, and invert them, as described there, to obtain $M_{\text{WD}}(f, p_{\text{rec}})$ and $\dot{M}(f, p_{\text{rec}})$ from the observables of Schaefer (2010). We note that p_{rec} is denoted by D in Hillman et al. (2016). The results are presented in Table 4, where the first column lists the year of the last eruption. For IM Nor, the recurrence period is uncertain (an eruption may have been missed), while for T Pyx, the last recurrence time was significantly larger than the average; hence for these two objects we list values obtained for two possible recurrence periods.

We note that both samples on which the mass and accretion rate distributions are based—the observational one and the theoretical one—are sparse. Hence statistically, the individual results have significant errors (we estimate $0.1M_{\odot}$ or so, based on deviations of assumed WD masses and accretion rates from the polynomial interpolation functions noted above). This is acceptable because the aim of this paper is to determine the nova WD mass *distribution*, rather than accurate individual masses. The few extant dynamical WD mass estimates (see below) have similar errors.

Table 4: RN: WD masses and accretion rates from observations (Schaefer 2010; Strope et al. 2010) and models

Observations			Modeling		
Nova	$f(\text{days})$	$p_{rec,obs}(\text{yr})$	$M_{\text{WD}}(M_{\odot})$	$\log \dot{M}(M_{\odot}/\text{yr})$	$m_{acc}(M_{\odot})$
T Pyx	329	19 (44)	1.23	-6.95 (-7.20)	2.04E-06 (2.74E-06)
IM Nor	424	82 (41)	1.21	-7.32 (-7.11)	3.87E-06 (3.07E-06)
CI Aql	429	24	1.21	-6.95	2.55E-06
V2487 Oph	52	18	1.35	-7.39	7.23E-07
U Sco	42	10	1.36	-7.29	5.26E-07
V394 CrA	65	30	1.34	-7.49	9.72E-07
T CrB	93	80	1.32	-7.68	1.65E-06
RS Oph	114	15	1.31	-7.14	1.04E-06
V745 Sco	19	21	1.40	-7.96	2.32E-07
V3890 Sgr	30	22	1.38	-7.69	5.09E-07

4.1. Comparison with WD masses derived from observations

There are only five direct, dynamical determinations of WD masses from observations in the literature. In Table 5 we compare our results with those five WD masses.

Table 5: Comparison of WD masses (in M_{\odot}) derived from observations and models

Nova	Model	Observation	Reference
V838 Her 1991	1.35	1.38 ± 0.13	Garnavich et al. (2018)
BT Mon 1939	0.95	1.04 ± 0.06	Smith et al. (1998)
RN U Sco	1.36	1.55 ± 0.24	Thoroughgood et al. (2001)
V603 Aql 1918	1.24	1.2 ± 0.2	Arenas et al. (2001)
DQ Her 1934	0.95	0.60 ± 0.07	Horne et al. (1993)

For 4 out of 5 cases - BT Mon, U Sco, V838 Her and V603 Aql - we find very good agreement between the WD masses derived directly from observations and our theoretical derivation. We also note that the ejected mass we calculate for BT Mon was derived from observations to be $\sim 3 \times 10^{-5} M_{\text{WD}}$ (Schaefer & Patterson 1983) , in very good agreement with the mass derived here.

DQ Her is a notable exception, where the most recent mass determination $0.60+/-$

$0.07 M_{\odot}$ (Horne et al. 1993) contrasts with our theoretical determination of $0.9 M_{\odot}$. The spectrographic data reduction is complex, as explained in detail by Horne et al. (1993). Two earlier estimates claim masses of $1.09 M_{\odot}$ (Robinson 1976) and $1.0 \pm 0.1 M_{\odot}$ (Hutchings et al. 1979). Horne et al. (1993) themselves report on a calculation with slightly less stringent assumptions that results in a higher WD mass, $0.68 \pm 0.1 M_{\odot}$. DQ Her is unusual as its WD is a very fast rotator (with a spin period of 71 s). Our own derivation may be an overestimate; when the critical pressure required for ignition is reached, the accreted column mass at the pole is lower than that at the equator. This means that the outburst will start declining earlier, implying a WD mass larger than it really is. In addition, DQ Her showed a deep dip in its light curve beginning 100 days after maximum.

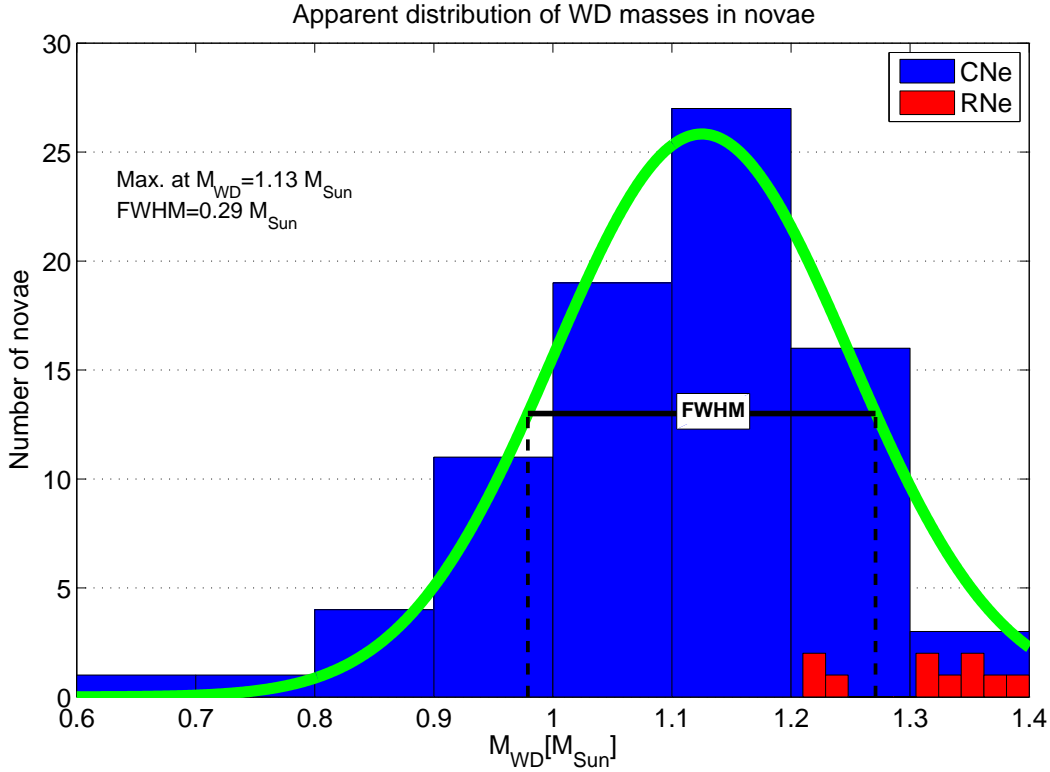


Fig. 2.— The frequency-averaged distribution of WD masses for 82 CN and 10 RNe. See text for details.

4.2. Comparison with WD masses derived by light-curve fitting

The data bases on which the present study is based are either purely observational or entirely theoretical. By combining them, as explained above, we were able to determine the

WD masses of observed novae. A completely different procedure that combines theory and observations in order to derive nova WD masses was proposed by Kato & Hachisu (1994), hereafter KH94, and has been used by them for individual objects ever since. As the KH94 mass estimates are derived with an entirely different methodology from that of this paper, it is interesting to compare them to the masses derived here. The KH94 method is based on fitting an optically thick wind solution, following the theory developed by Ruggles & Bath (1979), to the observed multi-band light curve corresponding to the mass-loss and decline phase of a nova. The parameters assumed in KH94 are the WD mass, the initial envelope mass, and its composition, disregarding prior evolution and the WD structure below the envelope. A series of steady state models with decreasing envelope mass is used to mimic the progression in time. The parameters are varied until agreement with the observed light curve is achieved. The WD masses obtained by the two methods of combining theory and observation are compared in Table 6.

Despite the inherent approximations and simplifications of each method, the agreement between them is acceptable for now. Future direct observational WD mass measurements will be essential to determine which method of WD mass derivation is more accurate.

4.3. Apparent distribution of WD masses and accretion rates

The distributions of WD masses and accretion rates that we derive are listed in Tables 1 and 2 and are shown in Figs. 2 and 3. The average nova WD mass is $1.13M_{\odot}$ and the average accretion rate $1.25 \times 10^{-9}M_{\odot}/\text{yr}$. We note that the average mass is in excellent agreement with the theoretical estimate of Ritter et al. (1991), who predict the mean WD mass, weighted by nova frequency (that is, the value determined directly by observations), to be found between 1.04 and $1.24 M_{\odot}$. The peak of the accretion rate distribution corresponds to $\dot{M} = 10^{-9}M_{\odot}/\text{yr}$, which is in excellent agreement with Townsley & Bildsten (2005), who argue, based on the distribution of orbital periods, that about 50% of CN occur in binaries accreting at $\dot{M} \approx 10^{-9}M_{\odot}/\text{yr}$.

In Fig. 4 we show the recurrence time distribution of our sample of 82 CN and 10 RNe. Recurrence times are determined by the amount of accreted mass required to trigger an outburst, which depends strongly on the WD mass (Prialnik & Kovetz 1995); they are inversely proportional to the accretion rate. The distributions of WD masses and accretion rates obtained for the observed sample do not reflect the true distributions within nova systems, since they are strongly biased by the outburst recurrence times.

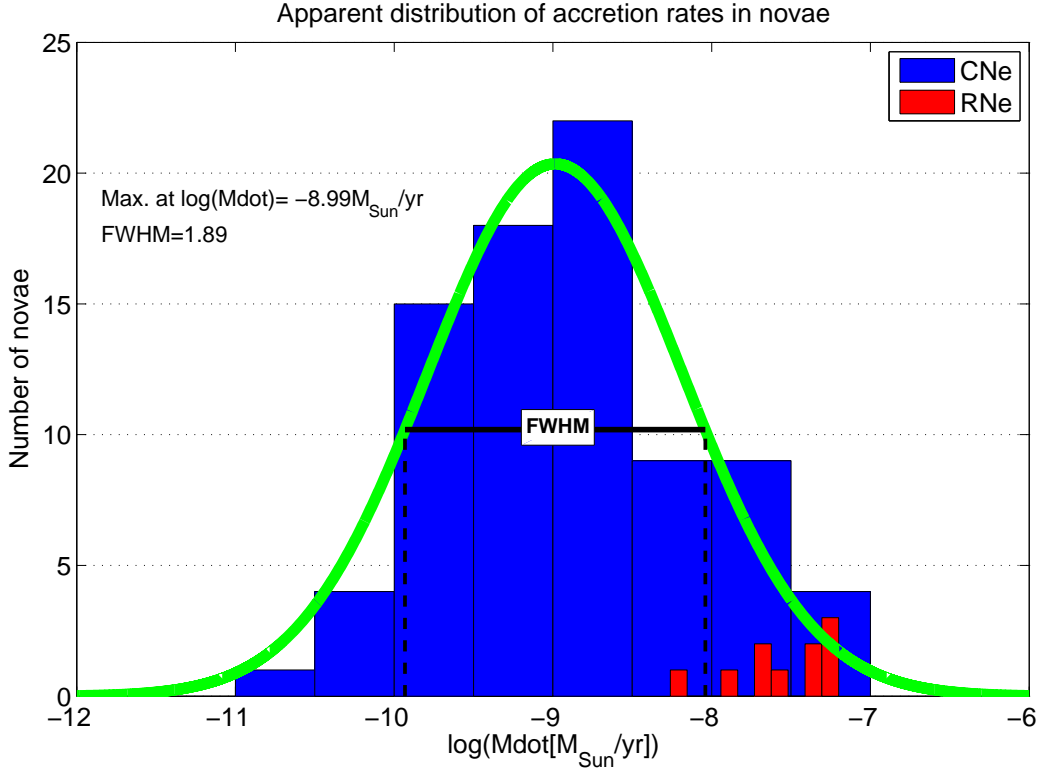


Fig. 3.— The frequency-averaged distribution of accretion rates for 82 CN and 10 RNe. See text for details.

5. Distribution of WD masses and accretion rates in novae

In this section we derive the true distributions of WD masses and accretion rates in nova systems, based on the sample of observed novae in Tables 1 and 2. The sample is assumed to be sufficiently large and randomly sampled that even quite rarely erupting novae are included. We note that, if they exist, extremely low mass transfer rate systems (i.e. “hibernating” cataclysmic binaries (Shara et al. 1986)) with $\dot{M} \leq 10^{-11} M_{\odot}/\text{yr}$ will be missed; only one such system - V1500 Cyg - is identified in Table 1.

Let x denote the WD mass and $P_1(x)$ the probability that the WD mass in a nova systems is x . By contrast, the probability that a WD from the observed sample has mass x will be denoted $P_{1,obs}(x)$. Let y denote the accretion rate (on logarithmic scale) and $P_2(y)$ – the probability that the accretion rate in a nova system is y . Similarly, the probability that a nova in the observed sample has accretion rate y (on logarithmic scale) will be denoted by $P_{2,obs}(y)$. The variables x and y may assume values within known intervals $[x_{min}, x_{max}]$ and $[y_{min}, y_{max}]$.

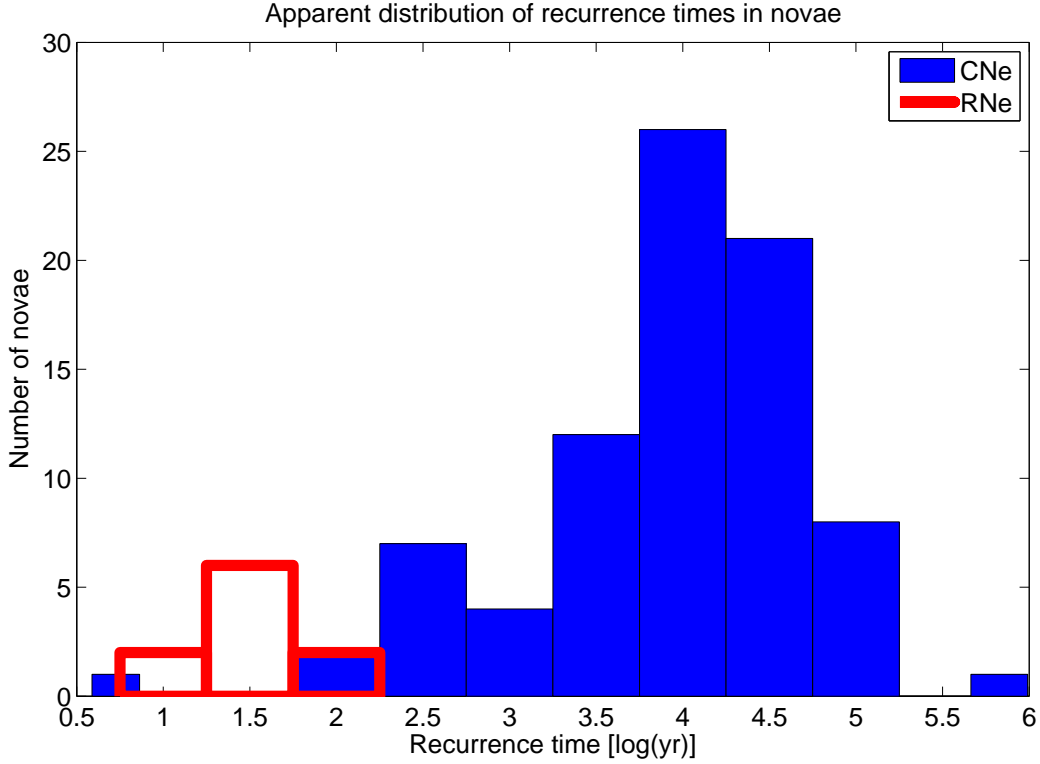


Fig. 4.— The distribution of recurrence times for 82 CN and 10 RNe. See text for details.

For the sample of N observed novae and the distribution of masses and accretion rates within them, we define the corresponding probabilities $P_{1,obs}(x)$ and $P_{2,obs}(y)$ as follows: if $N_{1,obs}(x)dx$ denotes the number of systems with masses in the range $[x, x+dx]$ and $N_{2,obs}(y)dy$ – the number of systems with accretion rates in the range $[y, y+dy]$, then

$$\begin{aligned} dN_{1,obs}(x) &= P_{1,obs}(x)dx \\ dN_{2,obs}(y) &= P_{2,obs}(y)dy \end{aligned} \quad (1)$$

and obviously,

$$\int_{x_{min}}^{x_{max}} P_{1,obs}(x)dx = \int_{y_{min}}^{y_{max}} P_{2,obs}(y)dy = N, \quad (2)$$

the total number of objects in the observed sample.

The difference between the actual mass and accretion rate distributions and the observed ones is due to different recurrence periods p_{rec} of nova outbursts, where the recurrent period is a function of both the WD mass and the accretion rate. This functional dependence, which we denote by $p_{rec} = f(x, y)$, is derived theoretically from the grid of models.

Now, the probability of observing a system with a WD mass x and an accretion rate y per unit time is proportional to the occurrence frequency p_{rec}^{-1} , hence the probabilities of observing systems of given mass or given accretion rate are given by

$$\begin{aligned} P_{1,obs}(x) &= P_1(x) \int_{y_{min}}^{y_{max}} \frac{1}{f(x, y)} P_{2,obs}(y) dy \\ P_{2,obs}(y) &= P_2(y) \int_{x_{min}}^{x_{max}} \frac{1}{f(x, y)} P_{1,obs}(x) dx . \end{aligned} \quad (3)$$

where the observed distributions are known. We can solve Eq.3 to obtain $P_1(x)$ and $P_2(y)$, either by assuming Gaussians for $P_{1,obs}(x)$ and $P_{2,obs}(y)$ or by discretization. We thus obtain relative distributions (that we normalize), namely, the shifts of the observed distribution with respect to the actual ones. Obviously, if the recurrence time is the same for all objects, the probability distributions will be equal. We apply this formalism to the sample of galactic novae by binning the WD mass range into n_x bins x_1, x_2, \dots, x_{n_x} and the accretion rates into n_y bins y_1, y_2, \dots, y_{n_y} . To each observed nova we assign a x_i value according to its corresponding mass bin and a y_j value, according to its corresponding accretion rate bin. We then calculate the function $f(x_i, y_j)$ according to a fit formula derived from the grid of models (in a similar way as we computed WD masses and accretion rates).

The number of objects in each mass bin x_i is denoted $N_{x,i}$ and the number of objects in each mass accretion bin, $N_{y,j}$, and hence

$$P_{1,obs}(x_i) = N_{x,i}/N \quad (4)$$

and similarly,

$$P_{2,obs}(y_j) = N_{y,j}/N . \quad (5)$$

Now, for each x_i and y_j , the integrals on the RHS of Eq.3 are replaced by the following sums, respectively:

$$S_x(x_i) = \sum_{j=1}^{n_y} \frac{P_{2,obs}(y_j)}{f(x_i, y_j)} \quad \text{and} \quad S_y(y_j) = \sum_{i=1}^{n_x} \frac{P_{1,obs}(x_i)}{f(x_i, y_j)} , \quad (6)$$

where the summation includes all objects that fall into the WD mass bin x_i in the first case, and all objects that fall into the accretion rate bin y_j , in the second. This yields the original distributions $P_1(x_i) = P_{1,obs}(x_i)/S_x(x_i)$ and $P_2(y_j) = P_{2,obs}(y_j)/S_y(y_j)$, which we normalize, so that

$$\sum_{i=1}^{n_x} P_1(x_i) = 1 \quad \text{and} \quad \sum_{j=1}^{n_y} P_2(y_j) = 1 . \quad (7)$$

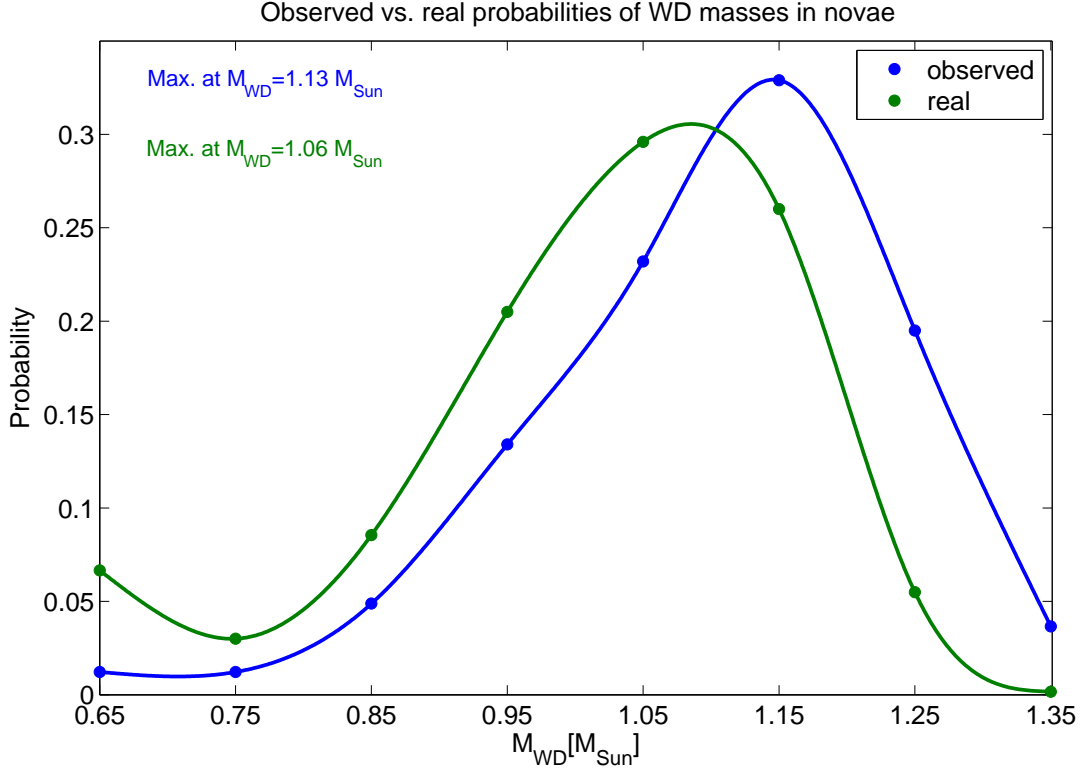


Fig. 5.— The real distribution of WD masses in nova systems. See text for details.

The results for the WD mass distribution, showing the shift with respect to the observed distribution are shown in Fig. 5. The accretion rate distribution, where the shift amounts to one order of magnitude, is shown in Fig. 6. The most probable WD mass is $1.13M_{\odot}$ while the average WD mass of the true distribution is $1.06M_{\odot}$. The true average accretion rate $1.3 \times 10^{-10} M_{\odot}/\text{yr}$.

6. Discussion and Conclusions

The frequency-averaged masses of WDs in CN and RNe have long been predicted to be much larger than those of field WD. We have used our extensive set of nova models to determine the relationships between WD mass, time to decline by 2 magnitudes, and outburst amplitude. These relationships have been used to deduce the masses of the WD in 82 Galactic CN.

We find that while the average CN mass of the Galactic novae is $1.13 M_{\odot}$, the frequency-

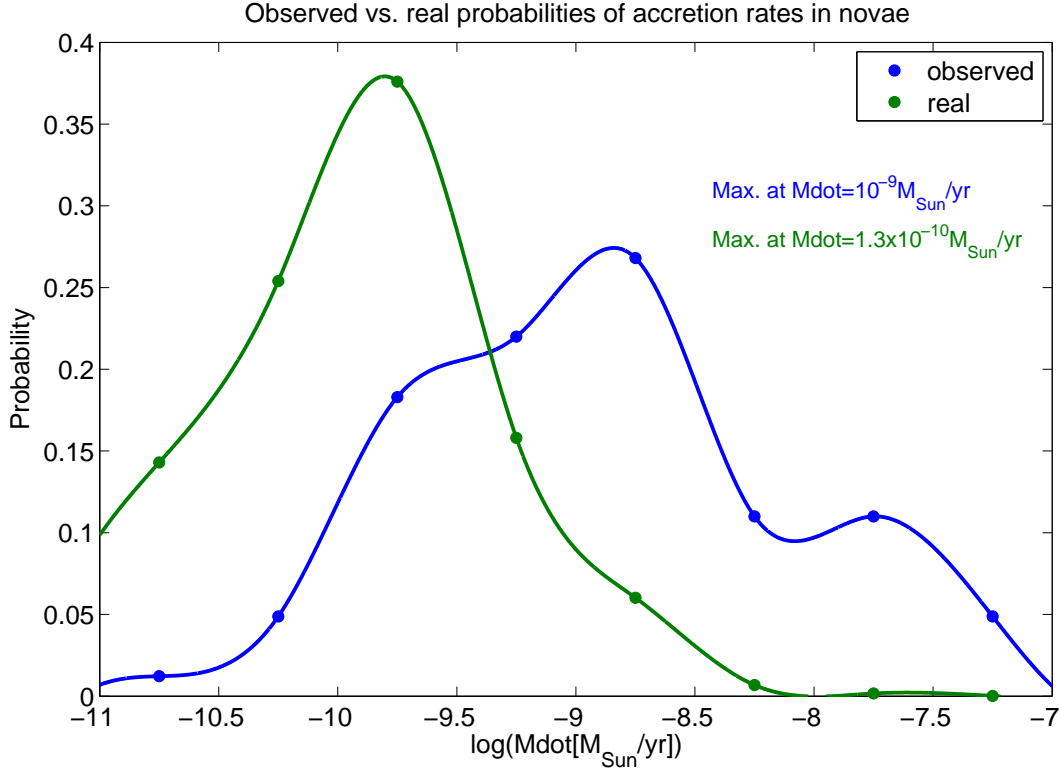


Fig. 6.— The real distribution of accretion rates in nova systems. See text for details.

averaged (true) CN mass is $1.06 M_{\odot}$, in very good agreement with population synthesis predictions. The mean mass of 10 recurrent novae is significantly larger, $1.31 M_{\odot}$.

The difference in WD mass between the frequency-averaged mass and the true average mass is modest - just $0.07 M_{\odot}$, so that the sharp discrepancy between field WD and nova WD masses remains in place, and important to understand. The true mass transfer rate, however, *is a full order of magnitude lower than the frequency-averaged rate*, (i.e. that corresponding to direct observation). The most frequent outbursts, detected most frequently, should occur in the highest \dot{M} systems. Here, for the first time, we are able to quantify the size of that observational bias.

We find that the longterm, true mass accretion rate of CN is remarkably low: $1.3 \times 10^{-10} M_{\odot}/\text{yr}$. All cataclysmic binaries transferring matter at this low rate experience dwarf nova eruptions. This is supportive of the view that mass transfer rates decline strongly in the centuries after nova eruptions, so that old novae undergo a metamorphosis to become dwarf novae for some or much of the millennia between nova eruptions. The four oldest old novae are all now observed to be dwarf novae (Shara et al. 2007, 2012; Miszalski et al. 2016;

Shara et al. 2017) surrounded by shells of ejected matter.

We determine the average mass accretion rates of the 10 known Galactic RN to be in the range 10^{-7} - 10^{-8} M_{\odot}/yr (with a mean of 4×10^{-8} M_{\odot}/yr).

Finally, we have determined the recurrence time distribution of Galactic novae. In addition to RN with recurrence times shorter than a century, we find a few CN which must erupt every few hundred years. However, the vast majority of CN recur on timescales of tens of millennia or longer. We note that in the sample of CN, that is novae for which only one outburst has been recorded, there are two objects with calculated recurrent times falling within the range of RNe (less than 100 yr): V1187 Sco and V4643 Sgr, both relatively recent and very fast novae. We predict that these are in fact RNe and the latter, at least, may erupt again in the near future.

MMS gratefully acknowledges the support of the late Ethel Lipsitz and Hilary Lipsitz, longtime friends of the AMNH Astrophysics department. He thanks J. Mikolajewska for very helpful suggestions concerning WD masses in recurrent novae.

REFERENCES

- Belczynski, K., & Mikolajewska, J. 1998, MNRAS, 296, 77
- Bergeron, P., Saffer, R. A., & Liebert, J. 1992, ApJ, 394, 228
- Canal, R., Ruiz-Lapuente, P., & Burkert, A. 1996, ApJ, 456, L101
- Chandrasekhar, S. 1931, ApJ, 74, 81
- Chandrasekhar, S. 1935, MNRAS, 95, 207
- Chen, H.-L., Woods, T. E., Yungelson, L. R., Gilfanov, M., & Han, Z. 2016, MNRAS, 458, 2916
- Darnley, M. J., Henze, M., Bode, M. F., et al. 2016, ApJ, 833, 149
- Darnley, M. J., Hounsell, R., Godon, P., et al. 2017, ApJ, 123, 123
- Faulkner, J., Flannery, B. P., & Warner, B. 1972, ApJ, 175, L79
- Ferrarese, L., Côté, P., & Jordán, A. 2003, ApJ, 599, 1302
- Gallagher, J. S., Hege, E. K., Kopriva, D. A., Butcher, H. R., & Williams, R. E. 1980, ApJ, 237, 55
- Garnavich, P., Kennedy, M., Littlefield, C., et al. 2018, AAS mtg 231 id 358.09
- Gehrz, R. D., Woodward, C. E., Helton, L. A., et al. 2008, ApJ, 672, 1167-1173
- Hachisu, I., & Kato, M. 2001, ApJ, 558, 323
- Hachisu, I., & Kato, M. 2007, ApJ, 662, 552
- Hachisu, I., & Kato, M. 2009, ApJ, 694, L103
- Hachisu, I., & Kato, M. 2010, ApJ, 709, 680
- Hachisu, I., & Kato, M. 2014, ApJ, 785, 97
- Hachisu, I., & Kato, M. 2015, ApJ, 798, 76
- Hachisu, I., & Kato, M. 2016, ApJ, 816, 26
- Hachisu, I., Kato, M., & Schaefer, B. E. 2003, ApJ, 584, 1008
- Han, Z., & Podsiadlowski, P. 2004, MNRAS, 350, 1301

- Henze, M., Darnley, M. J., Kabashima, F., et al. 2015, *A&A*, 582, L8
- Hillman, Y., Prialnik, D., Kovetz, A., Shara, M. M., & Neill, J. D. 2014, *MNRAS*, 437, 1962
- Hillman, Y., Prialnik, D., Kovetz, A., & Shara, M. M. 2016, *ApJ*, 819, 168
- Horne, K., Welsh, W. f., & Wade, R. A. 1993, *ApJ*, 410, 357
- Hutchings, J. B., Cowley, A. P., & Crampton, D. 1979, *ApJ*, 232, 500
- Iben, I., Jr., & Tutukov, A. V. 1985, *ApJS*, 58, 661
- Kasliwal, M. M., Cenko, S. B., Kulkarni, S. R., et al. 2011, *ApJ*, 735, 94
- Kato, M., & Hachisu, I. 1994, *ApJ*, 437, 802
- Kato, M., Hachisu, I., & Cassatella, A. 2009, *ApJ*, 704, 1676
- Kato, M., Saio, H., Hachisu, I., & Nomoto, K. 2014, *ApJ*, 793, 136
- Kepler, S. O., Pelisoli, I., Koester, D., et al. 2016, *MNRAS*, 455, 3413
- Kovetz, A., & Prialnik, D. 1985, *ApJ*, 291, 812
- Livio, M. 1992, *ApJ*, 393, 516
- Maoz, D., Mannucci, F., & Nelemans, G. 2014, *ARA&A*, 52, 107
- Mikolajewska, J., & Shara, M. M. 2017, *arXiv:1702.08732*
- Miszalski, B., Woudt, P. A., Littlefair, S. P., et al. 2016, *MNRAS*, 456, 633
- Nelson, L. A., MacCannell, K. A., & Dubeau, E. 2004, *ApJ*, 602, 938
- Paczynski, B., & Zytlow, A. N. 1978, *ApJ*, 222, 604
- Pagnotta, A., & Schaefer, B. E. 2014, *ApJ*, 788, 164
- Politano, M. 1996, *ApJ*, 465, 338
- Prialnik, D., Shara, M. M., & Shaviv, G. 1978, *A&A*, 62, 339
- Prialnik, D., Livio, M., Shaviv, G., & Kovetz, A. 1982, *ApJ*, 257, 312
- Prialnik, D., & Kovetz, A. 1995, *ApJ*, 445, 789
- Provencal, J. L., Shipman, H. L., Høg, E., & Thejll, P. 1998, *ApJ*, 494, 759

- Ritter, H., Politano, M., Livio, M., & Webbink, R. F. 1991, *ApJ*, 376, 177
- Ritossa, C., Garcia-Berro, E., & Iben, I., Jr. 1996, *ApJ*, 460, 489
- Robinson, E. L. 1976, *ApJ*, 203, 485
- Ruggles, C. L., & Bath, G. T. 1979, *Å*, 80, 97
- Schaefer, B. E. 2010, *ApJS*, 187, 275
- Schaefer, B. E., & Patterson, J. 1983, *ApJ*, 268, 710
- Shafter, A. W., Rau, A., Quimby, R. M., et al. 2009, *ApJ*, 690, 1148
- Shara, M. M., Prialnik, D., & Shaviv, G. 1980, *ApJ*, 239, 586
- Shara, M. M. 1981, *ApJ*, 243, 926
- Shara, M. M., Livio, M., Moffat, A. F. J., & Orio, M. 1986, *ApJ*, 311, 163
- Shara, M. M., Martin, C. D., Seibert, M., et al. 2007, *Nature*, 446, 159
- Shara, M. M., Mizusawa, T., Wehinger, P., et al. 2012, *ApJ*, 758, 121
- Shara, M. M., Doyle, T. F., Lauer, T. R., et al. 2016, *ApJS*, 227, 1
- Shara, M. M., Doyle, T., Lauer, T. R., et al. 2017, *ApJ*, 839, 109
- Shara, M. M., Iłkiewicz, K., Mikołajewska, J., et al. 2017, *Nature*, 548, 558
- Sion, E. M. 1999, *PASP*, 111, 532
- Smith, D. A., Dhillon, V. S., & Marsh, T. R. 1998, *MNRAS*, 296, 465
- Starrfield, S. G., Sparks, W. M., & Truran, J. W. 1975, *Memoires of the Societe Royale des Sciences de Liege*, 8, 425
- Starrfield, S., Sparks, W. M., & Truran, J. W. 1986, *ApJ*, 303, L5
- Strope, R. J., Schaefer, B. E., & Henden, A. A. 2010, *AJ*, 140, 34
- Townsley, D. M., & Bildsten, L. 2005, *ApJ*, 628, 395
- Tremblay, P.-E., Cummings, J., Kalirai, J. S., et al. 2016, *MNRAS*, 461, 2100
- Whelan, J., & Iben, I., Jr. 1973, *ApJ*, 186, 1007

Williams, R. E., Woolf, N. J., Hege, E. K., Moore, R. L., & Kopriva, D. A. 1978, ApJ, 224, 171

Williams, R. E. 1982, ApJ, 261, L77

Yaron, O., Prialnik, D., Shara, M. M., & Kovetz, A. 2005, ApJ, 623, 398

Young, P., & Schneider, D. P. 1980, ApJ, 238, 955

Table 6: Comparison of WD masses with those obtained by light-curve fitting

Paper	Object	M_{WD} from K&H	M_{WD} this paper	t_2 days ⁽¹⁾
Hachisu & Kato (2016)	V1668 Cyg ^(a)	0.98	1.16	11
	V1974 Cyg ^(b)	0.98	1.12	19
	QU Vul	0.96	1.04	20
	V351 Pup	1.00	1.19	9
	V382 Vel ^(c)	1.23	1.21	6
	V693 CrA	1.15	1.15	10
Hachisu & Kato (2015)	PW Vul	0.83	1.01	44
	V705 Cas	0.78	1.05	33
	RR Pic	0.5-0.6	0.95	73
	HR Del	0.5-0.55	0.84	167
	V723 Cas	0.5-0.55	0.77	263
Hachisu & Kato (2014)	V1500 Cyg ^(d)	1.20	1.09	2
	GK Per ^(e)	1.05	1.22	6
	V603 Aql	1.20	1.24	5
Hachisu & Kato (2010)	V382 Vel 1999 ^(c)	1.23	1.21	6
	V4743 Sgr 2002	1.15	1.22	6
	V1494 Aql 1999	1.13/1.06/0.92	1.20	8
	V2467 Cyg 2007	1.11/1.04/0.90	1.20	8
	V5116 Sgr 2005	1.07/1.0/0.85	1.22	12
	V574 Pup 2004	1.05	1.15	12
	V1974 Cyg 1992 ^(b)	1.05	1.12	19
	V1668 Cyg 1978 ^(a)	0.95	1.16	11
	V1500 Cyg 1975 ^(d)	1.15	1.09	2
Hachisu & Kato (2009)	V2491 Cyg	1.32/1.3/1.27	1.26	4
	V1493 Aql	1.2/1.15/1.1	1.18	9
	V2362 Cyg	0.75/0.7/0.65	1.19	9
Kato et al. (2009)	V838 Her	1.35±0.02	1.35	1
Hachisu & Kato (2007)	GK Per ^(e)	1.15±0.05	1.22	6
	V5115 Sgr	1.20±0.1	1.20	7
	V5116 Sgr	0.90±0.1	1.22	12
Hachisu et al. (2003)	Cl Aql	1.2±0.05	1.21	25
Hachisu & Kato (2001)	T CrB	1.37	1.32	4
	RS Oph	1.35/1.377	1.31	7
	V745 Sco	1.35	1.4	
	V3890 Sgr	1.35	1.38	6
	U Sco	1.37	1.36	1
	V394 CrA	1.37	1.34	

⁽¹⁾ from Strope et al. (2010), ^{(a),(b),(c),(d),(e)} multiple entries